Journal of the Physical Society of Japan
Vol. 71, No. 2, February, 2002, pp. 504–508

Quasielastic Neutron Scattering of Liquid $Te_{50}Se_{50}$ in the Semiconductor-to-Metal Transition Range

Ayano CHIBA, Yoshinori OHMASA, Makoto YAO*,
Oleg PETRENKO[1] and Yukinobu KAWAKITA[2]

Department of Physics, Graduate School of Science, Kyoto University, Kyoto 606-8502
[1]*Rutherford Appleton Laboratory, Chilton, Didcot OX11 0QX, U.K.*
[2]*Department of Physics, Faculty of Science, Kyushu University, Fukuoka 810-8560*

(Received May 15, 2001)

We have carried out neutron scattering experiments for liquid $Te_{50}Se_{50}$ at 700 K (semiconducting regime), 900 K (transition regime) and 1100 K (metallic regime). The quasielastic scattering peak is comparatively narrow at the peak positions of $S(Q)$. A remarkable increase in the peak width is observed near the first minimum of $S(Q)$, when the semiconductor-to-metal transition occurs. Since the first peak of $S(Q)$ in this system proves to mainly reflect the inter-chain correlation and the second peak to the intra-chain correlation, the observed broadening may suggest frequent bond-switching between the chains in the metallic regime.

KEYWORDS: liquid, tellurium, selenium, semiconductor-to-metal transition, neutron scattering, dynamic structure, interchain correlation
DOI: 10.1143/JPSJ.71.504

1. Introduction

In the solid state, both selenium and tellurium are semiconductors composed of helical chains in which each atom is bonded to two adjacent atoms by covalent bonds. In the liquid state, however, they exhibit very different properties from each other. Liquid Te (l-Te) exhibits metallic properties in contrast to liquid Se (l-Se) in which the helical chain structure is more or less preserved. In 1995, it was revealed that l-Te has a twofold coordinated structure with two kinds of covalent bonds: one is normal covalent bond and the other is elongated owing to strong inter-chain coupling.[1,2)]

It is well known that Te and Se form liquid mixtures in the whole concentration range. In the liquid Te–Se mixtures, a semiconductor-to-metal (S–M) transition is induced by raising temperature and the transition temperature increases with the Se-concentration, as shown in Fig. 1.[3–5)] The S–M transition is accompanied by a structural change from a Se-like loosely packed structure to a Te-like densely packed structure. In the S–M transition region, various thermodynamic anomalies such as sound velocity[6–8)] and specific heat[9–11)] were observed.

On the contrary, very little has been studied on their dynamic aspects. Although neutron scattering experiments for l-Te[1)] and liquid $Te_{70}Se_{30}$[12)] have been done to investigate the dynamic properties influenced by the S–M transition, the former, which is metallic above the melting point, could be changed to a semiconductor in a strongly supercooled state, and the latter has the S–M transition range near the melting point, as shown in Fig. 1, and hence the measurements were done in comparatively narrow temperature range. Furthermore, both of them were measured in a very limited range of the momentum Q space, and conclusive results have not been obtained yet. In the present study, we have carried out neutron scattering experiments for liquid $Te_{50}Se_{50}$, in which one can clearly distinguish between the semiconducting regime and the metallic regime by temperature. In addition, anomalous sound attenuation is recently found in the S–M transition range,[13)] which implies that a slow-dynamics with a nanosecond time scale may occur due to the S–M transition.

From the viewpoint of experimental technique, Te–Se mixtures are very favorable for neutron scattering due to its high coherent scattering cross-section compared with the incoherent one. The coherent scattering provides not only the self part but also the distinct part of the scattering law, from which information on the cooperative motion can be extracted.

In this paper, we restrict ourselves to study the quasielastic part of the dynamic structure factor $S(Q, E)$ and investigate how the dynamic properties are influenced by the S–M transition in and around picosecond time scale. The purpose of this paper is to publish new experimental results and to establish a simple microscopic scenario to understand the results.

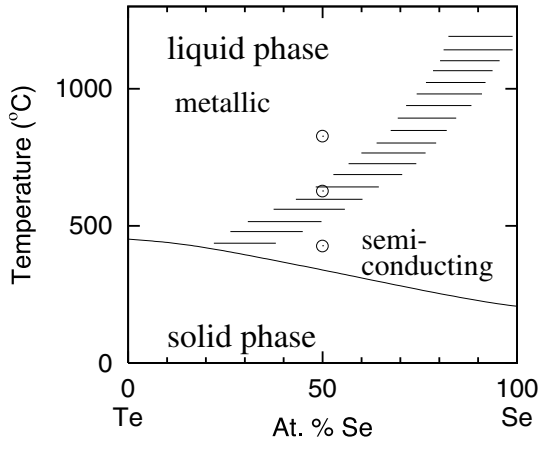

Fig. 1. Phase diagram of Te–Se system. The solid line is the liquidus curve, and the hatching indicates the semiconductor-to-metal transition region. The temperatures and the concentration at which neutron scattering experiments were carried out are denoted by open circles.

*Corresponding author.

2. Experimental

Neutron scattering experiments were performed on the MARI spectrometer in the ISIS facility of the Rutherford Appleton Laboratory, UK. MARI is a chopper spectrometer which covers a wide range of energy-momentum E–Q space. The incident energy was set to 40 meV in order to cover a reasonable kinematical range at low wave vectors without degrading substantially the resolution in energy transfers. The achieved energy resolution was about 0.7 meV, estimated from the vanadium-standard-sample run as the half-width at half maximum (HWHM) of the elastic peak. $Te_{50}Se_{50}$ was sealed in a fused quartz L-shaped tube, and its main part has dimensions of 10 mm and 10.6 mm in the inner and outer diameters, respectively, as shown in Fig. 2. The geometry of the niobium heating element is horizontal and cylindrical. The fused quartz tube was placed perpendicularly to the incident beam. The measurements were carried out at 700 K (semiconducting regime), 900 K (transition regime) and 1100 K (metallic regime). Scattering from an empty fused quartz cell and the background including niobium heater were also measured at 900 K.

The raw scattering data are shown for the scattering angles of 48° and 76° as a function of energy in Figs. 3(a) and 3(b), respectively. A sharp elastic peak due to (a) the fused quartz cell or to (b) the background including niobium heater is seen and a broad quasielastic peak is observed only for the sample. Note that Fig. 3 shows the raw scattering data not at constant Q but at constant scattering angles. In addition, they are not corrected for any effects such as resolution function and a detailed balance factor. These effects may result in apparent asymmetry of the quasielastic peak. The following formula were used to deduce the corrected scattering intensity from the sample, I_s, from observed scattering intensity I^{obs} for each counter:[15)]

$$I_s(E) = \frac{1}{A^s_{s+c}}\left\{[I^{obs}_{s+c}(E) - I^{obs}_b(E)] - \frac{A^c_{s+c}}{A^c_c}[I^{obs}_c(E) - I^{obs}_b(E)]\right\}, \quad (2.1)$$

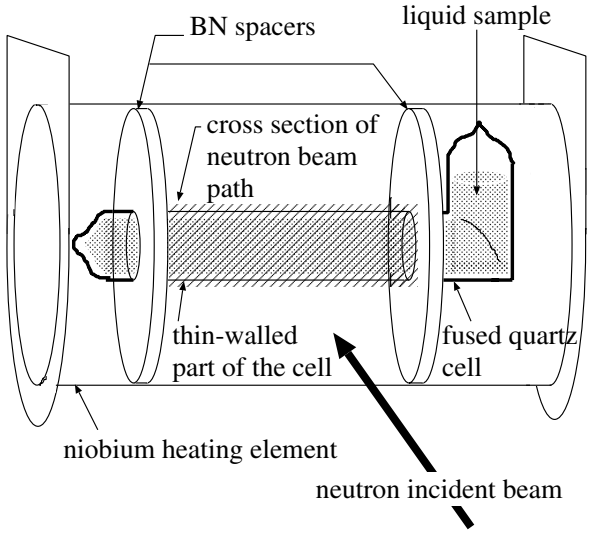

Fig. 2. High temperature apparatus for MARI spectrometer.

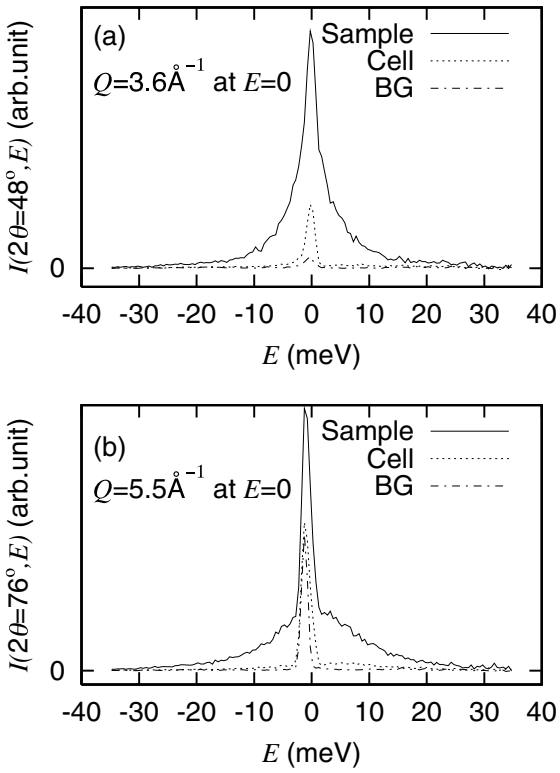

Fig. 3. Observed scattering intensity $I(2\theta, E)$ from liquid $Te_{50}Se_{50}$ encapsulated in a fused quartz cell, from empty cell and from background including niobium heater at the detecting angles of (a) 48° and (b) 76°.

where I^{obs}_i is the observed scattering intensity from the material i. The subscripts s, c and b denote the sample, the fused quartz cell and the background including niobium heater, respectively. A^j_i is the correction of the effect that the neutron scattered by the material j is absorbed by the material i, and was calculated by the method proposed by Paalman and Pings.[16)] In this correction we took the difference between absorption of the filled and empty containers into account.

The contributions of both quartz cell and niobium heater have no fundamental influence on the scattering of the liquid sample because the shape of the broad quasielastic peak is significantly different from the sharp elastic peaks of both quartz cell and niobium heater, as shown in Fig. 3. Since no sharp elastic peak is expected to be observed in the liquid sample, we have checked the validity of eq. (2.1). The contributions of both the cell and the heater could be properly subtracted except for 11 detecting angles out of 143 angles.

3. Results

Figure 4 shows a three-dimensional representation of the experimental dynamic structure factor $S(Q, E)$ of $Te_{50}Se_{50}$ at 700 K. A qualitative view of the variation with temperature can be seen from contour plots of the $S(Q, E)$ shown in Fig. 5. The blank areas in these figures correspond to the lack of data at several scattering angles, where the detectors are absent or do not work properly. It can be seen from Fig. 5 that the width of the quasielastic peak increases with both the momentum transfer Q and the temperature. Since $S(Q, E)$ is required to satisfy the relation

$$S(Q) = \int_{-\infty}^{\infty} S(Q,E)\mathrm{d}E, \tag{3.1}$$

we calculated the integrated intensity of $S(Q,E)$ over the energy transfer from -35 meV to 35 meV for each detector, as shown in Fig. 6. In the present experiments, we could measure $S(Q,E)$ in a wide range of the E-Q space, covering the first peak (i.e. 2 Å^{-1}), second peak (i.e. 3.5 Å^{-1}) and the third peak (i.e. 5.4 Å^{-1}) of $S(Q)$. The agreement with

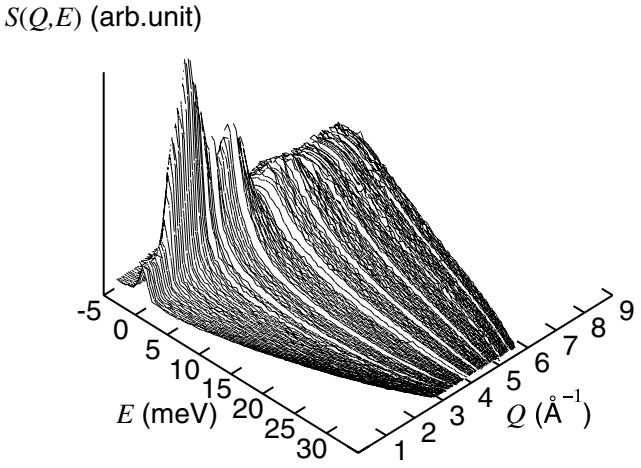

Fig. 4. Three-dimensional representation of the experimental dynamic structure factor of $Te_{50}Se_{50}$ at 700 K.

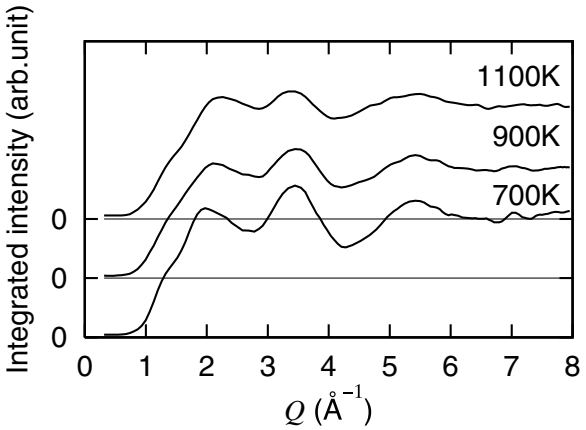

Fig. 6. Integrated intensity of $S(Q,E)$ for l-$Te_{50}Se_{50}$ at 700 K, 900 K and 1100 K over E-range as a function of momentum transfer Q at $E = 0$.

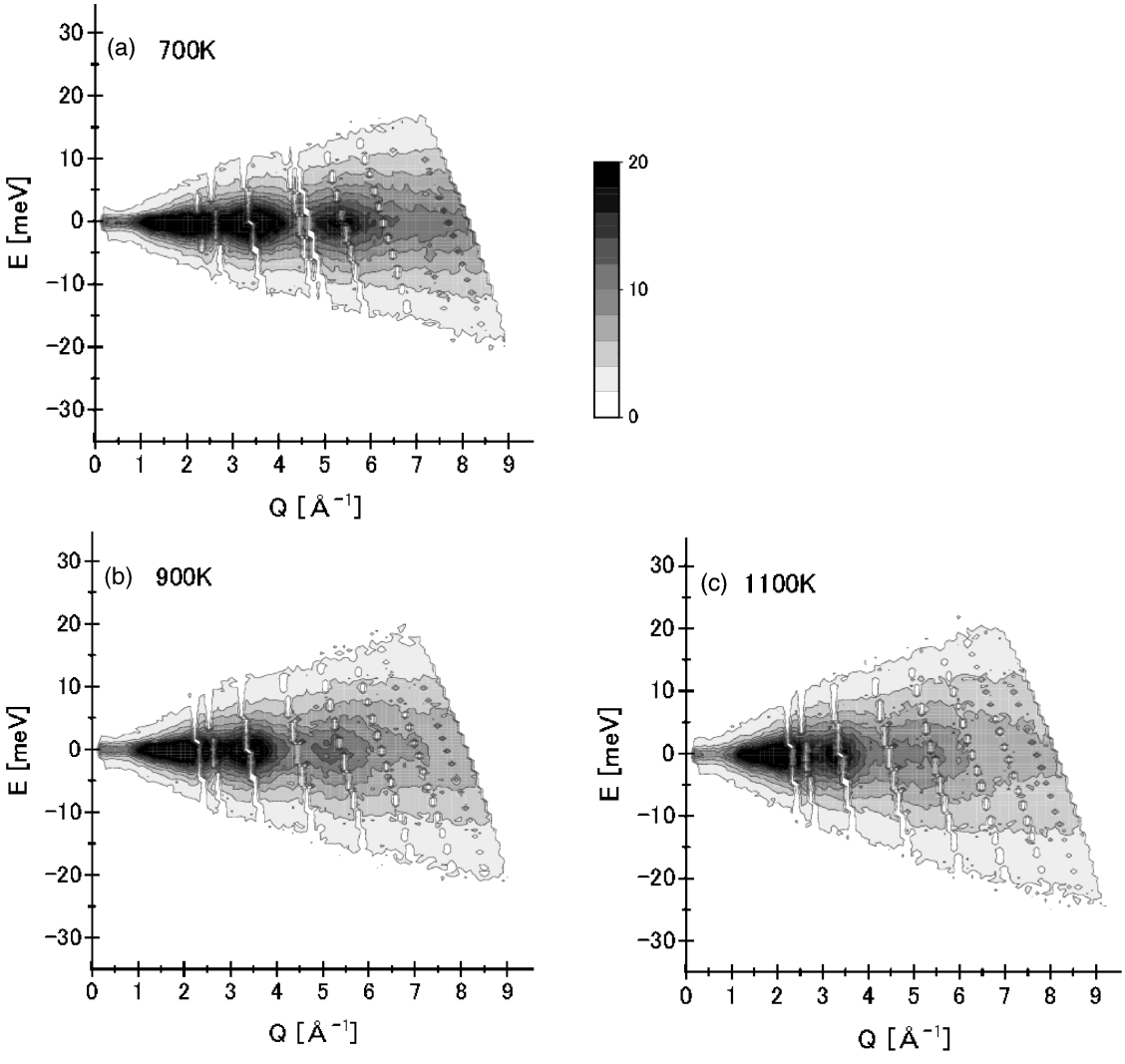

Fig. 5. Contour plots of $S(Q,E)$ for l-$Te_{50}Se_{50}$ at (a) 700 K, (b) 900 K and (c) 1100 K. The intensity is given in arbitrary units.

previously observed $S(Q)$ of similar composition and temperature[17–20] was good, especially in the point that the relative intensity of the first peak increases with the temperature, comparing with the intensity of the second peak. In this paper, we concentrate on the momentum transfer region from $0.5\,\text{Å}^{-1}$ to $6.5\,\text{Å}^{-1}$ in which the data was shown to be quite reliable, as shown in Fig. 6. Analysis of $S(Q,E)$ was carried out by a curve fitting procedure at $Q =$ constant with a Lorentzian function convoluted with a typical energy resolution function. The half-width at half-maximum, HWHM, of the quasielastic scattering peaks exhibit ''de Gennes narrowing'' at the peak positions of $S(Q)$ as shown in Fig. 7. The examples for the calculated curves are shown in Fig. 8 by solid lines.

4. Discussion

When the atoms have a long-range diffusive motion, which have a perfectly incoherent cross-section, HWHM of $S(Q,E)$ is related to the diffusion constant D as $\text{HWHM} = DQ^2$, which is so-called a DQ^2 law. In practice, however, each atom diffuses under the restriction of two covalent bonds. If the atoms move preserving the chain structure of the molecule, HWHM is expected to be much smaller than the DQ^2 law. Furthermore, because of the high coherent scattering cross-section of the Te–Se sample, HWHM contains information on the cooperative motion. At first we start from the simple DQ^2 law to understand the complex motion of the chain molecules.

Using Vineyard's approximation, the van Hove time correlation function $G(\boldsymbol{r},t)$ is given by

$$G(\boldsymbol{r},t) \approx G_{\text{s}}(\boldsymbol{r},t) + \rho \int g(\boldsymbol{r}')G_{\text{s}}(\boldsymbol{r}-\boldsymbol{r}',t)\text{d}\boldsymbol{r}' \qquad (4.1)$$

where $G_{\text{s}}(\boldsymbol{r},t)$ is the self-part of $G(\boldsymbol{r},t)$.[21] This implies that $\frac{F(Q,t)}{F(Q,0)} \approx F_{\text{s}}(Q,t) = \exp(-DQ^2t)$ in the hydrodynamic regime, where $F_{\text{s}}(Q,t)$ is the self-part of the intermediate scattering function $F(Q,t)$. In Fig. 9, HWHM/Q^2 of the quasielastic peaks for l-$Te_{50}Se_{50}$ at 700 K (semiconducting regime), 900 K (transition regime) and 1100 K (metallic regime) are calculated to extract cooperative motion for this coherent sample. The dips in the HWHM of the quasielastic peaks near the first, second and third peaks of $S(Q)$, i.e., near $2\,\text{Å}^{-1}$, $3.5\,\text{Å}^{-1}$ and $5.4\,\text{Å}^{-1}$, are partly caused by the de Gennes narrowing effect. A remarkable increase in the peak width is observed near the first minimum of $S(Q)$ (i.e. $2.5\,\text{Å}^{-1}$), when the S–M transition occurs, as shown in Fig. 9. This increase is very interesting because the HWHM is expected to narrow depending on the factor $S(Q)$ at a constant temperature, as shown by de Gennes,[14] and at the same time the oscillation of $S(Q)$ around 1 for this system is reduced by the temperature increase, as shown in Fig. 6 and earlier works.[17,20] That is, Fig. 9 shows that the oscillation of HWHM becomes prominent near $Q \sim 2.5\text{Å}^{-1}$ in the metallic regime in spite of the reduction of the oscillation of $S(Q) - 1$ in the regime. The origin of this unusual increase will hereinafter be discussed.

In the Te–Se system, the density fluctuations increase in the S–M transition region,[22] and it is also suggested that the concentration fluctuations may be induced in the transition region.[23] Since both of such thermodynamic fluctuations should appear in the low-Q range with relatively long relaxation time, the observed increase of HWHM near

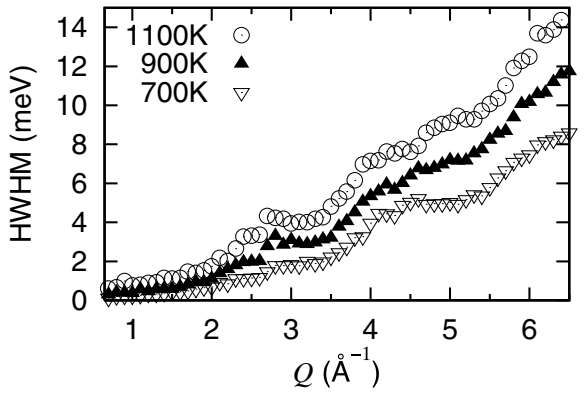

Fig. 7. Half-width at half-maximum of the quasielastic peaks as a function of Q.

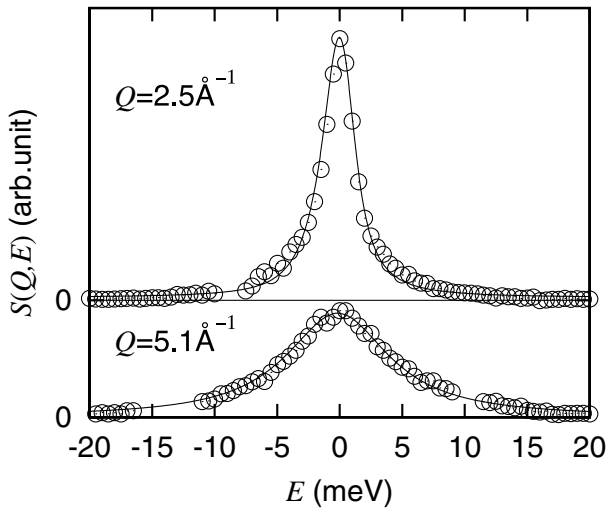

Fig. 8. Fits of the Lorentzian function convoluted with a typical energy resolution function to the $S(Q,E)$ for $Te_{50}Se_{50}$ at 700 K.

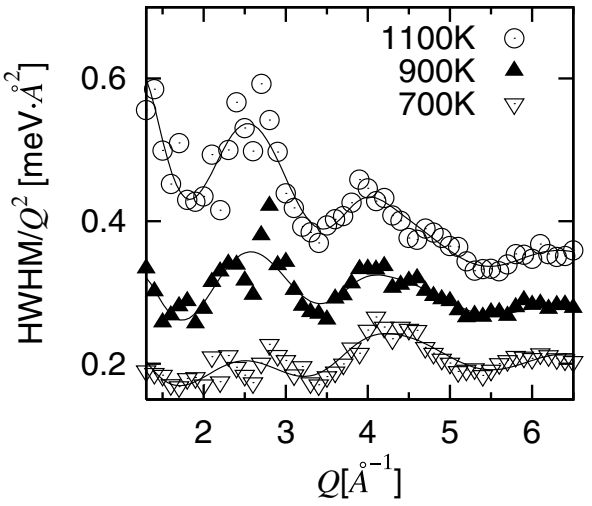

Fig. 9. HWHM/Q^2 of the quasielastic peaks for l-$Te_{50}Se_{50}$ at 700 K (semiconducting regime), 900 K and 1100 K (metallic regime). The lines in the figure are guides for the eyes.

2.5 $Å^{-1}$ is not directly related to them.

The first peak of $S(Q)$ in this system proves to be mostly related to the inter-chain correlation and the second peak to the intra-chain correlation.[1)] In the metallic regime, it is expected that the distinction between the inter- and intra-chain becomes less clear because of the thermal agitation. Consequently, the observed broadening may suggest frequent bond-switching between the chains in the metallic regime.

HWHM at the first minimum of $S(Q)$ in the metallic regime, about 4 meV as shown in Fig. 7, corresponds to the relaxation time of 0.16 ps. Hoshino and Shimojo carried out a MD simulation for l-Se at metallic regime (1770 K) and showed the time evolution of the local chain structure in subpicosecond time scale.[24)] They also showed that bond breaking and rearrangement of Se chains take place almost always with the interaction between Se chains. Although our sample and conditions like the temperatures are different from theirs, the possibility of frequent bond-switching between the chains in the metallic regime is consistent with their MD result. As a result, it is probable that the bond breaking and rearrangement of chains play an important role in the metallic region also in liquid Te–Se mixtures.

5. Summary

Neutron scattering measurements were carried out for liquid $Te_{50}Se_{50}$ at 700 K (semiconducting regime), 900 K (transition regime) and 1100 K (metallic regime). The width of the quasielastic peak exhibits ''narrowing'' at the peak positions of $S(Q)$. A remarkable increase in the peak width is observed near the first minimum of $S(Q)$ (i.e. 2.5 $Å^{-1}$), when the S–M transition occurs. The observed broadening may suggest frequent bond-switching between the chains in the metallic regime because the first peak of $S(Q)$ in this system proves to mainly reflect the inter-chain correlation and the second peak to the intra-chain correlation.

Acknowledgment

We would like to thank Dr. S. M. Bennington for discussions to prepare the experiments. We also acknowledge Prof. M. Arai for encouragement, and Dr. Y. Inamura for helpful advice on data analysis. This work was partially supported by a Grant-in-Aid on Scientific Research from the Ministry of Education, Culture, Sports, Science and Technology Japan (grant 10044101) and was carried out under the UK–Japan collaboration on neutron scattering. The experiments were carried out as a proposal RB11972 on MARI.

1) T. Tsuzuki, M. Yao and H. Endo: J. Phys. Soc. Jpn. **64** (1995) 485.
2) Y. Kawakita, M. Yao and H. Endo: J. Non-Cryst. Solids **250–252** (1999) 695.
3) J. P. Perron: Adv. Phys. **16** (1967) 657.
4) M. Yao, M. Misonou, K. Tamura, K. Ishida, K. Tsuji and H. Endo: J. Phys. Soc. Jpn. **48** (1980) 109.
5) H. Endo, K. Tamura and M. Yao: Can. J. Phys. **65** (1987) 266.
6) M. Yao, K. Suzuki and H. Endo: Solid State Commun. **34** (1980) 187.
7) K. Takimoto and H. Endo: Phys. Chem. Liq. **12** (1982) 141.
8) Y. Tsuchiya: J. Phys. Soc. Jpn. **60** (1991) 960.
9) S. Takeda, H. Okazaki and S. Tamaki: J. Phys. Soc. Jpn. **54** (1985) 1890.
10) Y. Tsuchiya: J. Phys. Soc. Jpn. **57** (1988) 3851.
11) F. Kakinuma and K. Suzuki: Metallkd. **84** (1993) 541.
12) M. Yao and H. Endo: J. Non-Cryst. Solids **205–207** (1996) 85.
13) M. Yao, N. Itokawa, H. Kohno, Y. Kajihara and Y. Hiejima: J. Phys.: Condens. Matter **12** (2000) 7323.
14) P. G. de Gennes: Physica **25** (1959) 825.
15) M. Bée: *Quasielastic Neutron Scattering* (Adam Hilger, Bristol and Philadelphia, 1988).
16) H. H. Paalman and C. J. Pings: J. Appl. Phys. **33** (1962) 2635.
17) R. Bellissent and G. Tourand: J. Non-Cryst. Solids **35&36** (1980) 1221.
18) W. Hoyer, B. Kunsch, M. Suda and E. Wieser: Z. Naturforsch. A **36** (1981) 880.
19) R. Bellissent: Nucl. Instr. Meth. **199** (1982) 289.
20) S. Takeda, S. Tamaki and Y. Waseda: J. Phys. Soc. Jpn. **55** (1986) 4283.
21) J.-P. Hansen and I. R. McDonald: *Theory of Simple Liquids* (Academic Press, London, 1986) 2nd ed.
22) M. Yao, K. Suzuki and H. Endo: Solid State Commun. **34** (1980) 187.
23) M. Misawa and K. Suzuki: J. Phys. C **8** (1980) 203.
24) F. Shimojo, K. Hoshino, M. Watabe and Y. Zempo: J. Phys.: Condens. Matter **10** (1998) 1199.